

# Stochastic numerical approach to the bearing capacity of adjacent footings on spatially variable soils

Research Article

Joanna M. Pieczyńska-Kozłowska\*

Faculty of Civil Engineering Department of Geotechnics, Hydrotechnics, Underground and Water Construction, Wrocław University of Science and Technology, Wrocław, Poland

Received 08 April 2025; Accepted 10 March 2026

**Abstract:** The interaction of adjacent footings in spatially variable soils presents significant challenges in geotechnical engineering, particularly when soil heterogeneity introduces uncertainty into foundation performance. Traditional deterministic methods provide valuable insights into bearing capacity (BC) and settlement behaviour; however, they capture the complex interactions arising from spatial variability. This study employs the random finite element method to investigate how anisotropic random fields affect the BC of adjacent footings. The problem is considered in three distinct soil types: perfectly cohesive, purely frictional, and cohesive-frictional. A series of numerical simulations is conducted to examine the effects of foundation spacing and the spatial variability of soil properties. Deterministic results indicate that BC increases at the critical spacing but gradually diminishes as the spacing increases further. Probabilistic analyses reveal that soil heterogeneity significantly impacts foundation behaviour, particularly in non-cohesive soils, where the coefficient of variation of BC is highly sensitive to spatial fluctuations. Reliability-based assessments reveal that failure probabilities vary significantly depending on soil type and correlation structure, underscoring the importance of stochastic modelling in geotechnical design. These findings contribute to the development of risk-informed design methodologies, highlighting the importance of modelling spatial variability using stationary random fields. As shown, such approaches enhance foundation reliability assessments and informed engineering decision-making.

**Keywords:** *Adjacent foundations • RFEM • Soil spatial variability • Probability of failure • Bearing capacity*

## 1. Introduction

The growing emphasis on sustainable development and the environmental impact of construction has led to increased attention to the reuse of existing structures, often with modifications to their intended purposes. In geotechnical engineering, this frequently necessitates enhancing the load-bearing capacity (BC) of existing foundations or constructing new foundations adjacent to existing structures. The behaviour of closely spaced foundations has long been a subject of interest, given its practical implications for urban development, infrastructure expansion, and the retrofitting of ageing foundations.

Unlike isolated footings, adjacent foundations exhibit interference, arising from the superposition of stress zones within the soil mass. Classical studies, such as those by Terzaghi [1] and Stuart [2], laid the groundwork for understanding interference effects between footings. In Terzaghi's [1] classical BC theory, as shown in Figure 1, three zones under a footing can be distinguished: (i) the triangular wedge directly beneath the footing, (ii) a logarithmic spiral zone radiating outward, and (iii) a passive Rankine zone. This interaction frequently results in the formation of a rigid soil block between the footings, which in turn enhances their BC compared to that of single foundations [2–4]

Stuart [2] has shown that overlapping potential failure mechanisms beneath interacting footings can enhance the BC of each footing, and suggested, based on equilibrium analysis, a performance efficiency factor ( $\zeta$ ) as the ratio of

\* E-mail: joanna.pieczynska-kozłowska@pwr.edu.pl

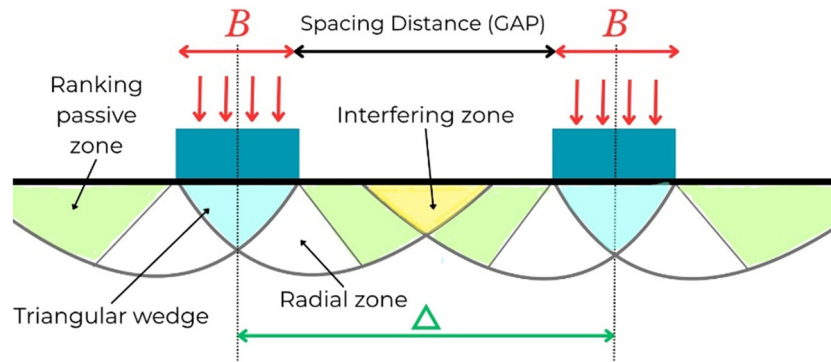


**Figure 1.** The scheme of the impact of adjacent foundations on each other.

the load carried by a footing neighbouring to the load capacity of another isolated footing of the same size:

$$\zeta = \frac{\text{The load carried by a foot neighbouring}}{\text{The load allowed on a separate foot of the same size}} \quad (1)$$

Stuart's approach suggested incorporating the efficiency factor into Terzaghi's BC equation:

$$q_u = qN_q\zeta_q + 0.5\gamma BN_y\zeta_y, \quad (2)$$

where  $\zeta_q$  and  $\zeta_y$  are correction factors for the BC components due to the interaction of neighbouring footings. Stuart observed that for non-cohesive soils with an internal friction angle ( $\phi$ ) of  $40^\circ$  and the centre-to-centre distance between footings ( $\Delta$ ) less than  $\Delta = 3B$  (Figure 1), the efficiency factor increased. The effect diminished as  $\phi$  decreased, with minimal interaction for purely cohesive soils.

Later experimental studies (Stuart, [2, 5]) also confirmed the development of an "inverse arch" mechanism between neighbouring footings, further increasing BC. In frictional soils, the efficiency factor varies between 1 and 2.6 for  $\Delta = 4B-5B$ , while in cohesive soils, the range is narrower (1-1.35 for  $\Delta = 3B$ ). Laboratory experiments conducted by Das and Larbi-Cherif [6] and Khing et al. [7] also demonstrated that closely spaced foundations can exhibit increased BC due to stress zone interactions. However, as the spacing between footings increases, their behaviour approaches that of isolated foundations. More recent experimental studies, including those by Schmüdderich et al. [8] and Eslami et al. [9], have extended these findings to more complex soil conditions, highlighting the role of soil type and loading conditions in foundation performance.

Previous investigations have also employed both analytical and numerical approaches to address the adjacent footing problem. Analytical studies have provided fundamental insights into failure mechanisms [10,11]. Upper-bound

and lower-bound formulations have been widely utilised to estimate ultimate loads under varying interference conditions [3,4]. In parallel, numerical modelling techniques have enabled the simulation of more complex scenarios.

Griffiths et al. [12] applied the Random finite element method (RFEM) to the BC problem of adjacent footings, accounting for spatially variable soil conditions, and demonstrated that even minor variations in soil properties can significantly affect failure mechanisms. The RFEM integrates random field theory established by Vanmarcke [13], with classical finite element analysis (FEM) and Monte Carlo simulation to account for spatial variability in geotechnical parameters. Soil properties are represented as random fields to ensure robust representation of soil heterogeneity, and multiple domain realisations are generated to statistically evaluate foundation behaviour under uncertainty. The role of soil variability has emerged as a critical factor in understanding foundation interactions. Studies such as those by Cafaro and Cherubini [14], Jha [15], or Puła and Chwała [16] have highlighted the influence of spatial correlation structures on soil strength and BC. Research by Kawa and Puła [17] expanded on these findings by incorporating three-dimensional probabilistic analyses and emphasising the need to account for anisotropic soil properties.

Most soil models assume weak stationarity, meaning the correlation (or covariance) function is translationally invariant. The autocorrelation function parameter is a scale of fluctuation (SOF), which represents the distance over which soil properties remain significantly correlated. The introduction of non-stationary soil models by Wu et al. [18], Shu et al. [19], and Choudhuri and Chakraborty [20] has further demonstrated that even modest fluctuations in soil properties can lead to significant variations in foundation behaviour.

While many studies have examined the impact of soil variability on single foundations, the influence of

stochastic soil properties on adjacent footings remains less explored. Recent efforts by Kawa [21], Alwalan [22], Ghazavi and Dehkordi [23], and Ghazavi et al. [24] have synthesised past research on foundation interference. The works of Pieczyńska-Kozłowska et al. [25] and Boru et al. [26] have made significant strides in addressing these challenges by integrating stochastic field analyses into foundation design methodologies. Additionally, reliability-based approaches, as presented by Moghaddam et al. [27] and Khajehzadeh and Keawsawasvong [28], have provided new perspectives on risk assessment in geotechnical engineering.

The aim of the present study is to advance the current understanding of the interaction between adjacent foundations by integrating stochastic modelling with soil-structure interaction analyses. By considering a range of soil types, including cohesive, frictional, and cohesive-frictional soils, and introducing anisotropic correlation structures, this research seeks to refine the probabilistic framework for foundation design in spatially variable conditions. A similar reliability-based framework for geotechnical design has been introduced for other foundation types in earlier works [29–31] and in standards, such as Eurocode 7 [32].

The study aims to quantify how spatial soil variability governs the interaction between adjacent foundations using advanced stochastic modelling. Its novelty lies in considering a wider range of soil types and spatial correlation structures, enabling a more comprehensive representation of soil conditions and a more rigorous assessment of the foundation interaction mechanisms.

The remainder of this study is organised as follows: Section 2 presents the theoretical background and methodology, detailing the RFEM framework and stochastic modelling approach. It also outlines the numerical model setup, including soil characterisation, boundary conditions, and loading schemes. Section 3 presents the results, focusing on the influence of foundation spacing and soil variability on BC, and discusses the implications of these findings. Finally, Section 4 concludes the study, summarising its key contributions and potential applications in reliability-based geotechnical design.

## 2. Methodology

### 2.1 Soil models and analytical calculations

In this study, three soil models were considered to represent a range of geotechnical conditions, including both idealised and natural materials. The first two approaches represented the behaviour of natural soils but were considered in this study as theoretical assumptions. Approach 1 – perfectly cohesive soil – represented a saturated undrained clay, where only total cohesion was considered (mean value: 36.3 kPa), and the internal friction angle was assumed to be zero. Approach 2 – purely frictional soil – simulated a clean, well-compacted sand under drained conditions, with an effective friction angle (mean: 35°) and negligible cohesion (1 kPa). The cohesive-frictional soil model (Approach 3) was developed using Taranto Blue Clay (TBC), a natural marine clay deposit in southern Italy. The effective strength parameters for TBC were derived from *in situ* and laboratory investigations reported by Cafaro and Cherubini [14]. These include a lognormally distributed cohesion with a mean value of 36.3 kPa and a bounded friction angle with a mean of 20°, ranging from 5° to 35°. This model reflects realistic variability observed in natural cohesive-frictional soils.

Initially, the analytical calculations for bearing capacities of isolated footings were performed using Terzaghi's formula. Two foundation widths,  $B = 1$  and 2 m, were adopted for the calculation, and are shown in Table 1. In principle, the width  $B = 2$  m corresponds to two foundations joined together.

The analytical resistances ( $q_a$ ) are estimated using resistance coefficients  $N_i$ , according to Eurocode 7. Total cohesion was used for the cohesive soil to reflect undrained behaviour (Approach 1). In contrast, effective parameters were applied in the frictional (Approach 2) and cohesive-frictional (Approach 3) cases to represent drained conditions. This classification enables a comparative analysis of foundation performance across different assumptions about soil type. The embedment of foundations was represented by a constant load next to the

	Analytical formula	BC value for $B = 1$ m	BC value for $B = 2$ m
Approach 1 – perfectly cohesive soil	$q_a = 5.12 c_u$	185.86 kPa	185.86 kPa
Approach 2 – purely frictional soil	$q_a = qN_q + 0.5B\gamma N_\gamma$	1108.41 kPa	1538.08 kPa
Approach 3 – cohesive-frictional soil	$q_a = cN_c + qN_q + 0.5B\gamma N_\gamma$	697.43 kPa	734.77 kPa

**Table 1.** Analytical values of resistance for each design approach.

Source: Author's contribution.

foundation ( $q$ ) equal to 19.0 kPa . In the case of a perfectly cohesive soil, the load  $q = 0$ . The results of the analytical calculations, assuming mean parameter values, are presented in Table 1. The BC of purely frictional soil shows the most significant dependence on foundation width.

## 2.2 Numerical deterministic simulations

Prior to the stochastic simulations, a series of preliminary finite element analyses were conducted to optimise both the mesh resolution and the displacement step parameters. The domain has been discretised into  $160 \times 40$  elements, each measuring  $0.25 \text{ m} \times 0.25 \text{ m}$ . The final domain dimensions were  $40 \text{ m} \times 10 \text{ m}$ , as illustrated in Figure 2. Such a domain of discretisation was assumed (as the effect of several tries) to ensure that no boundary effects were present. Two foundations with a dimension of  $B = 1 \text{ m}$  each were adopted for the study. As in the analytical examples, the 1 m embedment was modelled by applying a pressure of  $19 \text{ kN/m}^2$  to the soil surface (except in Case 1). The Mohr-Coulomb soil model was assumed for all calculations. The soil strength parameters were considered to be constant at their means presented in the previous subsection.

The elastic parameters were defined as follows: Young's modulus  $E = 36,000 \text{ MPa}$  and Poisson's ratio  $\nu = 0.29$ . This configuration enabled accurate modelling of stress redistribution between adjacent footings without artificial constraints, as confirmed by the displacement field presented in Figure 3. The figure illustrates node displacements for a deterministic case with footing spacings ranging from 0.9 to 8 m. Interaction between footings was observed for spacings up to 3 m, whereas for spacings greater than 4 m the foundations behaved independently. As evidenced by the deformation zones, the domain was sufficiently large in this case.

Additionally, a detailed sensitivity study was conducted to calibrate the displacement increment and convergence criteria for each numerical situation. The selected displacement increment step size ensured that, for large footing spacings ( $\text{GAP} = 8 \text{ m}$ ; Figure 3), the numerical results closely matched the analytical BC of a single footing with a width of  $B = 1 \text{ m}$  (as presented in Tables 1–3). The limit state was consistently reached within 10 computational steps, thereby balancing numerical stability and physical accuracy. Numerical simulations were performed using the FEM code developed by Fenton and Griffiths [33].

The final simulations were carried out over a wide range of footing spacings denoted by GAP parameter, from 0.25, 0.5, 0.75, 1.0, 1.5, 2.0, 2.5, 3.0, 4.0, 5.0, 6.0, 7.0, to 8.0 m. This range enabled a comprehensive assessment of interaction effects between adjacent foundations under various spatial configurations. The results and conclusions from this task are presented in the following sections.

## 2.3 Numerical probabilistic approach

All stochastic analyses were performed to describe soil strength parameters, namely, cohesion and friction angle, and following predefined statistical distributions using random fields. Random fields used in this study were generated using the Local Average Subdivision method, initially proposed by Fenton and Vanmarcke [34]. Numerical probabilistic simulations were conducted using the RFEM code developed by Fenton and Griffiths [33] and modified by the author to accommodate anisotropic correlation structures and site-specific soil variability [35]. The vertical SOF ( $\text{SOF}_y$ ) was fixed at 0.7 m. In contrast, the horizontal scale ( $\text{SOF}_x$ ) was a subject of parametric study, with values of 1, 10, and 100 m considered in the analysis. These values reflect typical depositional patterns and the geological processes that influence soil structure [36].

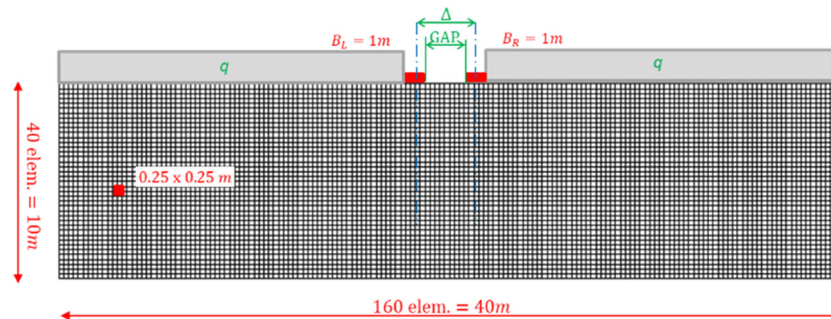
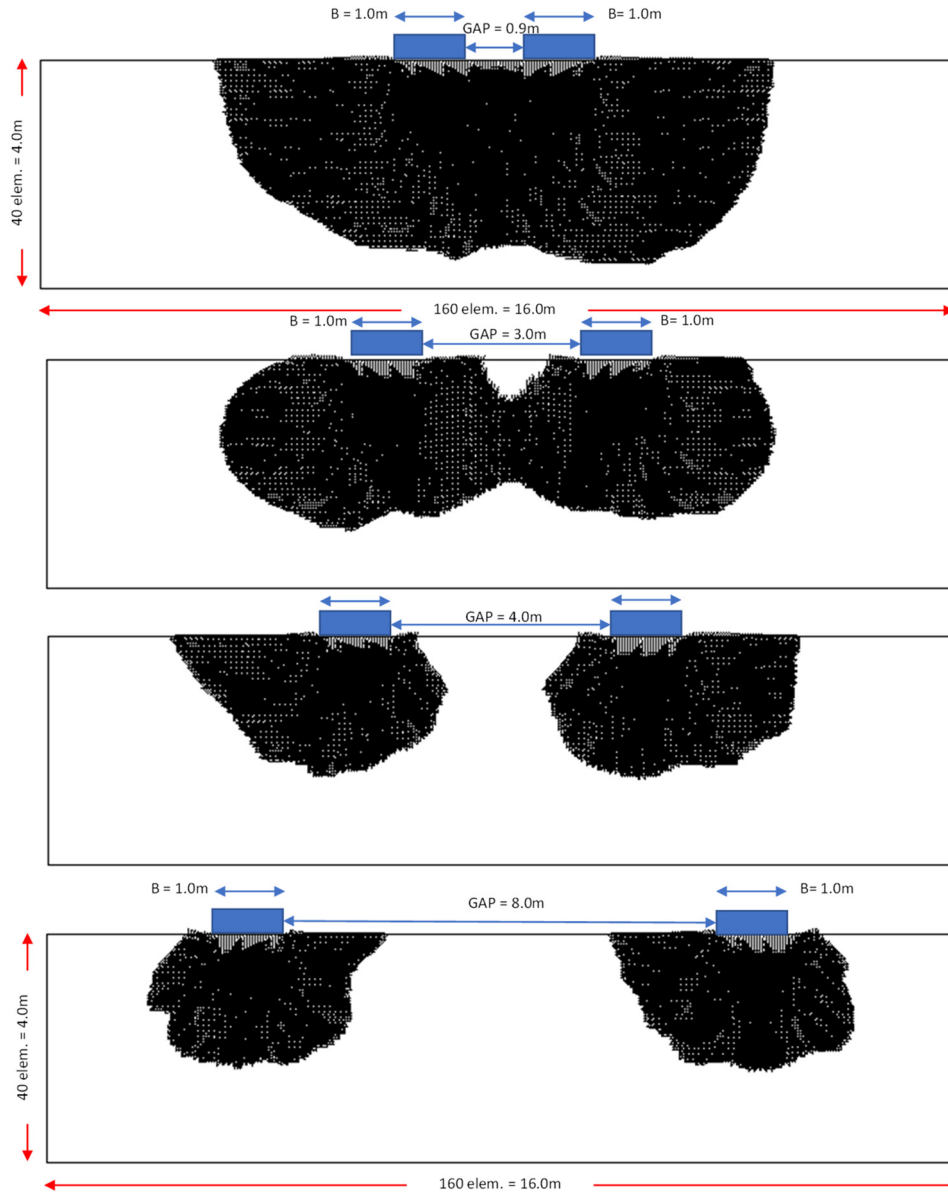


Figure 2. The adopted numerical model.

Source: Author's contribution.



**Figure 3.** Node displacement results for a deterministic task with foundation spacing 0.9–8 m.

Source: Author's contribution.

The selection of distributions was based on both empirical data and recent literature. Lognormal distributions were adopted for cohesion, reflecting its positively skewed nature in natural soils, as reported by field studies such as Cafaro and Cherubini [14] and by recent probabilistic analyses by Cami et al. [36]. For the friction angle, a bounded uniform distribution was used, consistent with observed variability ranges in natural deposits and contemporary stochastic modelling practices. The adopted distributions and statistical parameters for the three

considered cases are summarised in Tables 2–4 for the perfectly cohesive, purely frictional, and cohesive-frictional soil models, respectively.

To represent spatial correlation, anisotropic Markov-type autocorrelation functions were applied, defined as:

$$\rho(\tau) = \exp \left\{ - \sqrt{ \left( \frac{2\tau_x}{\text{SOF}_x} \right)^2 + \left( \frac{2\tau_y}{\text{SOF}_y} \right)^2 } \right\}. \quad (3)$$

	Mean value	Standard deviation	Distribution
Cohesion (c)	36.3 kPa	19.6 kPa	Lognormal
Friction angle ( $\phi$ )	—	—	Deterministic
Unit weight ( $\gamma$ )	—	—	Deterministic

**Table 2.** Soil parameters for a perfectly cohesive approach. Source: Author’s contribution.

	Mean value	Standard deviation	Distribution	Distribution parameters
Cohesion (c)	1 kPa	—	Deterministic	
Friction angle ( $\phi$ )	35°	—	Bounded	$\phi_{\min} = 25^\circ$
Unit weight ( $\gamma$ )	19 kN/m <sup>3</sup>	—	Deterministic	$\phi_{\max} = 45^\circ$

**Table 3.** Soil parameters for non-cohesive approach. Source: Author’s contribution.

Each probabilistic simulation scenario was performed using 500 realisations, a number determined through convergence testing to ensure stability of the mean BC across trials. This framework enabled a robust assessment of the influence of spatial variability on foundation performance under varying soil conditions and footing configurations.

The numerical results obtained in this study also allowed for a simple reliability analysis of adjacent footings. The results are interpreted in terms of the reliability index ( $\beta$ ) and compared against analytical benchmarks, providing insight into the adequacy of traditional design assumptions under realistic variability conditions. Generally, the probability of failure ( $p_f$ ) is defined as

$$p_f = P[R < S] = \Phi(-\beta), \quad (4)$$

where  $R$  is the resistance (e.g. BC) and  $S$  is the load effect. The reliability index ( $\beta$ ) is related to  $p_f$  via the standard normal distribution with  $\Phi$  denoting the cumulative distribution function of the standard normal distribution. Eurocode 7 does not prescribe a single target value for  $\beta$  but recommends values depending on the consequence class and design situation. For ultimate limit states, the reliability index corresponds to the probability of failure and is approximately  $p_f \sim 10^{-4}$ . In present study probability of failure is assumed as

$$p_f = \Phi(-\beta) = P[q < q_{a,d}], \quad (5)$$

where  $q_{a,d}$  represents the analytical BC ( $q_a$ , taken from Table 1 as the reference value), divided by the safety factor (FS). Result of stochastic analysis are also presented in Section 3.

### 3. Results and discussion

The section is divided into three sub-sections. The first sub-section presents the results of deterministic numerical analyses. The second sub-section presents the results of stochastic numerical analyses. Finally, the third sub-section presents the probabilistic results obtained based on reliability parameters.

#### 3.1 Results of numerical deterministic approach

The results of the performed deterministic numerical analysis are presented in Figure 4. Across soil types, the results show pronounced differences in both the magnitude and the nature of BC responses. For perfectly cohesive soils (Figure 4a), the analytical BC remains essentially constant regardless of footing width, which is consistent with classical theory. However, numerical results indicate a slight increase as adjacent footings are brought closer

	Mean value	Standard deviation	Distribution	Distribution parameters
Cohesion (c)	36.3 kPa	19.6 kPa	Lognormal	
Friction angle ( $\phi$ )	20°	—	Bounded	$\phi_{\min} = 5^\circ$
Unit weight ( $\gamma$ )	19 kN/m <sup>3</sup>	—	Deterministic	$\phi_{\max} = 35^\circ$

**Table 4.** Soil parameters for the cohesive-friction soil approach (TBC).

Source: Author’s contribution.

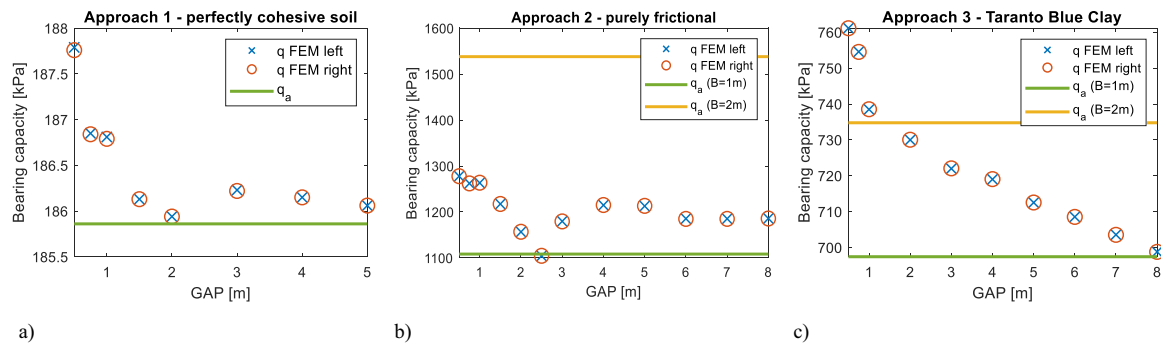


**Figure 4.** Analytical and numerical results for deterministic values of soil parameters for each approach: (a) ideal cohesive, (b) purely frictional, and (c) TBC.

Source: Author’s contribution.

together – an effect attributable to localised interaction not captured by analytical solutions. This subtle increase becomes noticeable when the distance between foundations is less than 1 m, suggesting that, even in perfectly cohesive conditions, spatial proximity can modestly enhance load BC. Still, the results are within 1% of the analytical solution, which raises doubts about whether the differences are not solely due to numerical error.

In purely frictional soils (Figure 4b), the analytical model predicts a strong dependence on footing width, with BC increasing significantly for wider foundations (as shown in Table 1). Nevertheless, numerical simulations show that the BC of two closely spaced footings does not exceed that of a single, wider footing, which may potentially arise from partial overlap of stress zones beneath adjacent foundations. The most substantial impact of foundation width on BC, and the most significant increase due to proximity, is observed when foundations are located closer than 1.5 m to each other. Notably, even at a minimal spacing of 0.25 m, the BC does not match that of a single foundation with  $B = 2$  m, underscoring the limitations of simple superposition in frictional soils. This interaction effect, in which proximity increases BC,

is consistent with the findings of Stuart [2] and Rybak and Konderla [11] and supports the validity of the numerical model used in the present study.

For the natural cohesive-frictional TBC (Figure 4c), the behaviour is more complex. Both the width of the foundation and the GAP between adjacent foundations significantly influence BC. Remarkably, when foundations are placed less than 1 m apart, the average BC can exceed that of a single foundation with double the width ( $B = 2$  m). Numerical results for closely spaced footings can even exceed the analytical value for a single isolated footing, suggesting a synergistic interaction effect that is entirely neglected in deterministic analytical models.

Differences preclude a direct comparison of absolute bearing capacities across soil types and foundation geometries. Figure 5a–c presents the normalised charts from Figure 4 to facilitate comparison of results across soil types. By expressing all results relative to the analytical BC of a single footing of width  $B = 1$  m for each soil type, the normalised plots enable a direct, dimensionless comparison of interaction effects across fundamentally different soils. This approach isolates the influence of foundation spacing and

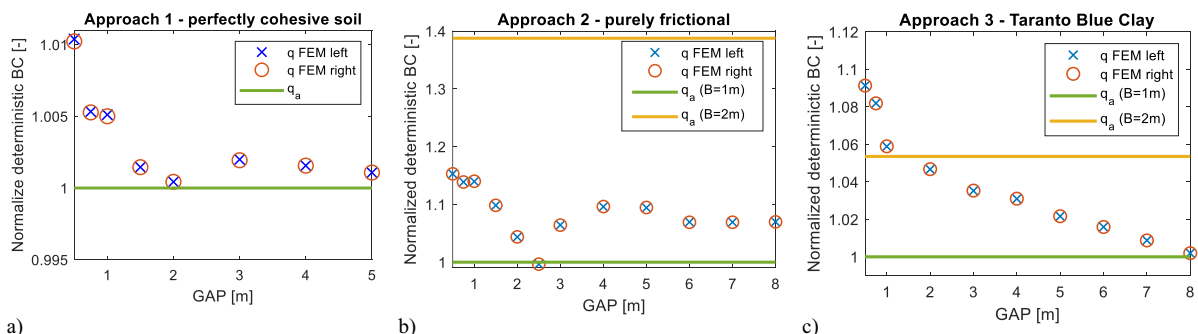


**Figure 5.** Normalised analytical and numerical results for deterministic values of soil parameters for each approach: (a) ideal cohesive, (b) purely frictional, and (c) TBC.

Source: Author’s contribution.

soil behaviour from the confounding effects of absolute strength, allowing for a more precise assessment of how spatial interactions modify the expected performance.

As a result of normalising the outcomes, an increase in BC of up to 15% is observed for foundations spaced 0.5 m apart in Approach 2. In Approach 3, the increase is approximately 10%, which is 5% higher than the BC of a single foundation with a weight of 2 m, whereas in Approach 1, it remains close to 1%. This enhancement does not evolve uniformly with increasing spacing. In Approach 3, the strengthening effect diminishes almost linearly with increasing distance. In contrast, in Approach 2, the BC decreases until the spacing reaches approximately 2.5B, after which it rises again to 8% for larger foundation spacing. This effect is not readily apparent and warrants further analysis. This comparative perspective underscores that the magnitude and even the direction of interaction effects are not universal but depend strongly on the underlying soil mechanics. For engineering design, this means that the potential benefits or drawbacks of placing foundations in proximity cannot be inferred from one soil type to another without careful consideration of the specific context.

### 3.2 Results of probabilistic numerical approach

The results of probabilistic analyses performed using RFEM are shown in Figures 6 and 7. Figure 6 illustrates the mean BC for probabilistically modelled soil parameters across three Approaches: (1) perfectly cohesive, (2) purely frictional, and (3) TBC. The results reveal distinct patterns for each case. The results in Figure 6 are normalised under the same conditions as in the previous subsection, by dividing the adequate analytical value from Table 1. In Approach 1 (Figure 6a), the mean BC is approximately 20% lower than the analytical value, indicating a significant

reduction due to spatial variability in cohesion. For Approach 3 (Figure 6c), the mean values are also lower, but the reduction does not exceed 10% of the analytical mean for  $B = 1$  m. Notably, when the gap between foundations is 1 m or less, the mean BC increases above the nominal value.

The non-cohesive (purely frictional) soil (Figure 6b) exhibits the most pronounced effect of spatial variability: for small gaps (0.25–1.0 m), the mean BC almost mirrors the deterministic results, while for gaps greater than 1 m, the mean values are slightly lower than their deterministic counterparts. The influence of the  $SOF_x$  on the mean BC is minimal, as evidenced in Figure 6.

Figure 7 shows the coefficient of variation (COV) for each Approach, which indicates a stronger relationship with SOFs. For  $SOF_x = 1$  m, the COV is consistently lower, regardless of the soil type. At larger scales ( $SOF_x = 10$  and 100 m), the COV values are similar, with variability generally increasing with scale. Furthermore, the COV exhibits fluctuations for gaps less than 1 m, independent of the soil model adopted.

A further point of interest is the dependence of COV on soil type. The highest COV is observed in the perfectly cohesive soil (Figure 7a), while the purely frictional soil (Figure 7b) displays the smallest COV. The natural soil (TBC, Figure 7c) presents intermediate values. This pattern suggests that cohesion variability directly influences the variability in the BC of adjacent foundations.

To synthesise the effect of soil type on the observed results, the author introduces a global Stuart reinforcement index ( $\zeta_G$ ), defined as the ratio of the mean BC from both foundations to the analytical BC for a single footing (equation 6).

$$\zeta_G = \frac{\text{Mean BC from both foundations}}{\text{Analytical BC value for a single footing}} \quad (6)$$

Figure 8 presents the global efficiency factor values for all considered approaches. The analytical factor suggested

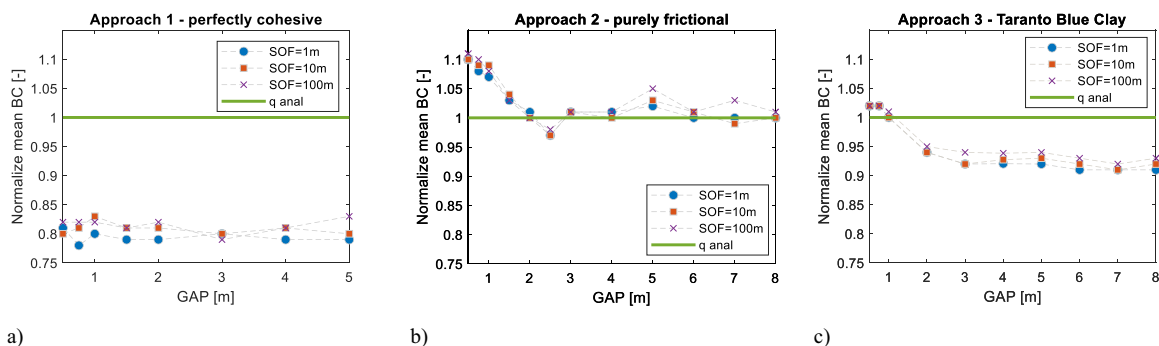
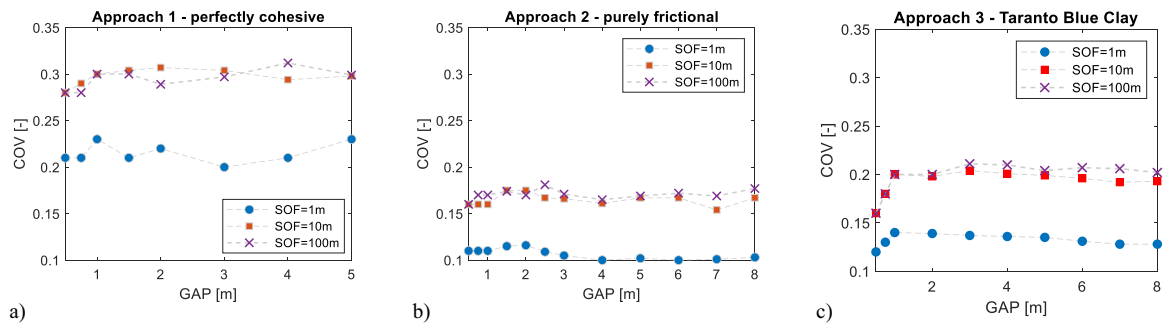


Figure 6. Mean BC for probabilistic values of soil parameters for each approach: (a) ideal cohesive, (b) purely frictional, and (c) TBC. Source: Author's contribution.



**Figure 7.** BC COV for probabilistic values of soil parameters for each approach: (a) perfectly cohesive, (b) purely frictional, and (c) TBC. Source: Author’s contribution.

by Stuart (1963) was in the range of 1–2.6 with axial spacing  $\Delta$  from  $4B$  to  $5B$  ( $GAP\ 5B-6B$ ) for purely frictional soils (as Approach 2), while for cohesive soils (like Approach 1), the range of factor was 1–1.35 for  $\Delta = 3B$  ( $GAP = 4B$ ). In the current analysis, bearing-capacity reinforcement is evident for GAPs less than  $2B$ ; in the probabilistic context, the magnitude of this reinforcement for natural soil under Approach 3 does not exceed 10%.

In Approach 2, the gain is most pronounced, reaching up to 20%. Conversely, cohesive soil demonstrates a reduction in the coefficient of up to 20%, regardless of the mutual position of the foundations.

### 3.3 Probability of failure

The probability of failure for adjacent shallow foundations, as illustrated in Figure 9, is evaluated using equation

5 under two principal design assumptions regarding the threshold values. First, with the values of  $q_{a,d}$ , and second,  $q_{a,d}$  multiplied by the Stuart coefficient ( $\zeta$ , Figure 8). Each row in Figure 9 corresponds to a specific soil type: Approach 1 (Figure 9a and b), Approach 2 (Figure 9c and d), and Approach 3 (Figure 9e and f). Each subfigure in Figure 9 depicts the relationship between probability of failure and GAP for two sets of results: values based on the analytical BC divided only by FS, represented by lines with markers, and values where the analytical BC is divided by FS and further multiplied by the Stuart coefficient obtained for each approach, represented by markers only. In each set, three values of SOF were considered.

A previous study by the author [25] demonstrated that the probability of failure strongly depends on the selected FS value, and that this safety level directly affects the estimation of the reliability index ( $\beta$ ). As illustrated in the Figure 9a, c and e the probability of failure exceeds 5% when  $FS = 1$ . That

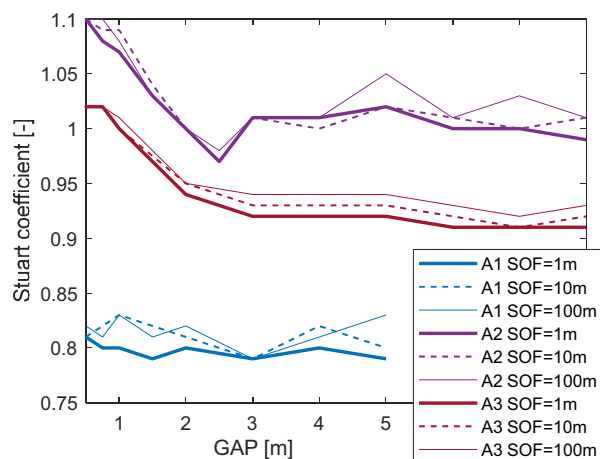
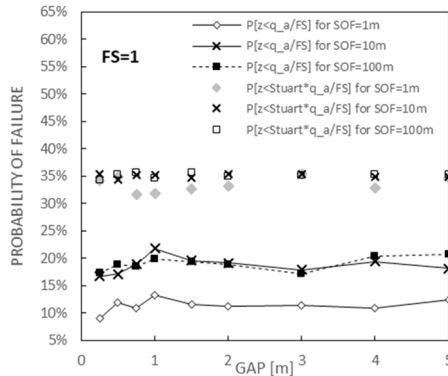
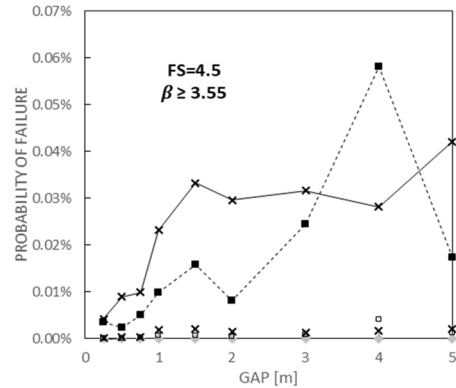


**Figure 8.** Performance efficiency factor for all approaches (A1 – Approach 1 – perfectly cohesive; A2 – Approach 2 – purely frictional; A3 – Approach 3 – TBC). Source: Author’s contribution.

Approach 1 –  
Perfectly  
cohesive soil

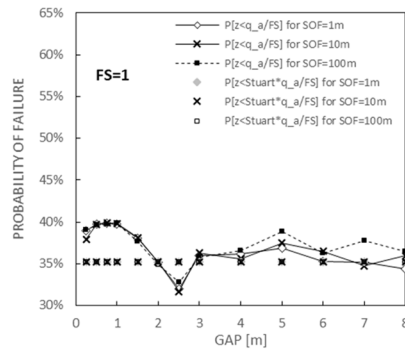


(a)

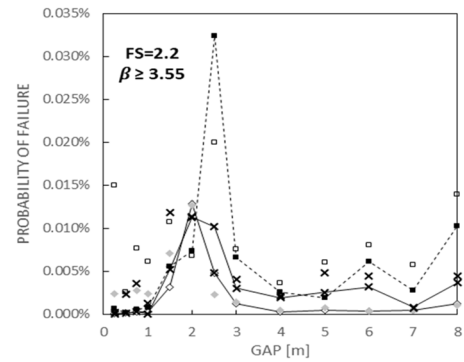


(b)

Approach 2 –  
Purely  
frictional soil

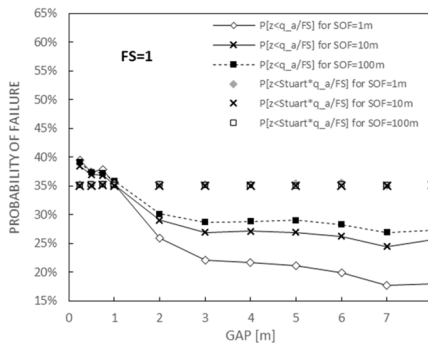


(c)

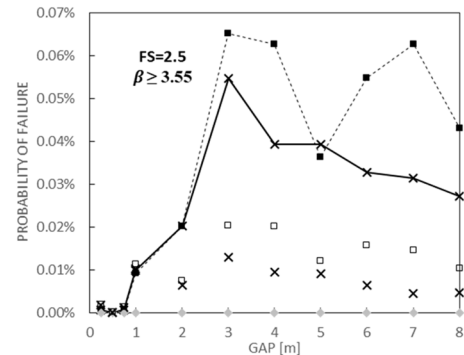


(d)

Approach 3 –  
cohesive-  
frictional soil  
(Taranto Blue  
Clay)



(e)



(f)

**Figure 9.** Probability of failure. (a and b) Approach 1 – perfectly cohesive soil, (c and d) Approach 2 – purely frictional soil, and (e and f) Approach 3 – cohesive-frictional soil (TBC).

Source: Author's contribution.

situation corresponds to a reliability index beta of around 0.5. To achieve a failure probability of  $p_f \sim 10^{-4}$ , as recommended in Eurocode 7, the reliability index must exceed  $\beta \geq 3.55$ . This requirement necessitates adopting different FS values for each soil type and approach, reflecting their inherent variability and associated reliability demands, as represented by column (2) in Figure 9b, d, and f.

Under the baseline scenario (FS = 1), a strong correlation is observed between failure probability and mean BC (as shown in Figure 6). When the Stuart coefficient is applied, the probability of failure stabilises at approximately 35% for all soil types, regardless of the correlation structure or relative foundation position.

For Approach 1 – perfectly cohesive soils (Figure 9b), achieving the target reliability index  $\beta \geq 3.55$  required a

FS = 4.5. In this case, the probability of failure approaches zero when the Stuart coefficient is included, indicating a highly conservative design. However, if the limit value is based solely on the standard analytical capacity (without the Stuart adjustment), the influence of spatial correlation becomes more pronounced, underscoring the importance of accounting for soil variability in reliability assessments.

In contrast, for Approach 2 (Figure 9d), the required SF to achieve  $\beta \geq 3.55$  is significantly lower (FS = 2.2). Here the effect of the Stuart coefficient is less pronounced, whereas the impact of the correlation structure is more pronounced. As the scale of fluctuation increases, so does the probability of failure in both scenarios. The highest failure probabilities are observed for GAPS between 1 and 3 m, indicating that interaction effects are most significant within this range under variable soil conditions.

For Approach 3 (Figure 9f), the effect of the correlation structure dominates. With a small fluctuation scale (SOF = 1 m), the probability of failure remains close to zero in both scenarios. As SOF increases, failure probability rises, particularly when the Stuart coefficient is applied, highlighting the soil's sensitivity to spatial variability and interaction effects. A particularly noteworthy observation is the influence of GAP on failure probability. Across all soil types, the failure probability increases sharply for GAP values between 0 and 3 m, reflecting strong interaction effects at close distances. For spacings greater than 3 m, the probability of failure stabilises or decreases slightly. This indicates that foundations begin to behave independently, and the interaction effect diminishes. Such a trend reinforces earlier findings that adjacent footings exhibit significant load-bearing interaction when placed in proximity; however, beyond a particular spacing, this effect wanes, and the probability of failure approaches that of isolated foundations.

## 4. Conclusion

This study sought to quantify the effects of spatial soil variability on the interaction between adjacent shallow foundations, to enhance the representation of subsoil heterogeneity using anisotropic random fields, and to broaden the scope of analysis by considering a wide range of soil types and spatial correlation structures, in contrast to previous research. The study shows that the magnitude and direction of interaction effects depend strongly on the arrangement of the foundation. The results presented indicate that spatial variability in soil parameters markedly

influences both the mean and the variability of BC, particularly for relatively closely spaced foundations.

In perfectly cohesive soils (Approach 1), the mean BC under probabilistic modelling was observed to be approximately 20% lower than the analytical value. In contrast, for natural cohesive-frictional soils (Approach 3), the reduction did not exceed 10%. For purely frictional soils (Approach 2), the proximity-induced amplification of BC was present but did not exceed 15%, even at minimal spacing.

The probability of failure increased sharply for GAPS below 3 m, reaching up to 35% when the SF was unity. The probability stabilised as foundations began to behave more independently. In cases such as the Stuart index, the probability of failure remains high at 35%. Achieving a reliability index consistent with Eurocode 7 recommendations required substantially higher SFs in cohesive soils than in frictional soils, reflecting the differing levels of uncertainty and risk. For practical design, this necessitates tailoring SFs and investigation strategies to the specific soil type and variability. The evaluation of potential beneficial or adverse interaction effects, especially for foundations spaced less than 3 m apart. These findings underscore the limitations of deterministic design or modifications based solely on Stuart's coefficient and highlight the need for probabilistic approaches that account for anisotropic variability.

Future research should extend this framework to a three-dimensional reliable geological model of the subsoil to validate the approach through large-scale field data. Such developments will support safer, more resilient foundation systems under complex ground conditions. Ultimately, the adoption of advanced stochastic approaches supports the development of safer, more economical, and more resilient foundation systems in complex ground conditions.

## References

- [1] Terzaghi, K. (1943). *Theoretical soil mechanics*. Wiley.
- [2] Stuart, J. G. (1962). Interference between foundations, with special reference to surface footings in sand. *Géotechnique*, 12(1), 15–25. doi: 10.1680/geot.1962.12.1.15.
- [3] Kumar, J., & Ghosh, P. (2007). Ultimate bearing capacity of two interfering rough strip footings. *International Journal of Geomechanics*, 7(1), 53–62.
- [4] Pal, A., Ghosh, P., & Majumder, M. (2017). Interaction effect of two closely spaced skirted strip foundations

- in cohesionless soil using upper-bound limit analysis. *International Journal of Geomechanics*, 17(2), 06016022.
- [5] Myslivec, A., & Kysela, Z. (1969). Effect of adjacent foundations on bearing capacity. *Acta Technica Academiae Scientiarum Hungaricae*, 64(1–2), 183.
- [6] Das, B. M., & Larbi-Cherif, S. (1983). Bearing capacity of two closely spaced shallow foundations on sand. *Soils and Foundations*, 23(1), 1–7. doi: 10.3208/sandf1972.23.1.
- [7] Khing, K. H., Das, B. M., Yen, S. C., Puri, V. K., & Cook, E. (1992). Interference effect of two closely-spaced shallow strip foundations on geogrid-reinforced sand. *Geotechnical Geological Engineering*, 10, 257–271. doi: 10.1007/BF00880704.
- [8] Schmüderich, C., Lavasan, A. A., Tschuchnigg, F., & Wichtmann, T. (2020). Bearing capacity of a strip footing placed next to an existing footing on frictional soil. *Soils and Foundations*, 60(1), 229–238. doi: 10.1016/j.sandf.2020.03.002.
- [9] Eslami, A., Afshar, D., Moghadasi, H., & Akbarimehr, D. (2024). Numerical and experimental investigations of the interference effect of adjacent buildings on sand and fill deposits. *International Journal of Civil Engineering*, 22(5), 723–738.
- [10] Lavasan, A., Ghazavi, M., Blumenthal, A. V., & Schanz, T. (2018). Bearing capacity of interfering strip footings. *Journal of Geotechnical and Geoenvironmental Engineering*, 144(3), 04018003.
- [11] Rybak, J., & Konderla, P. (1993). Influence of spacing on bearing capacity of shallow foundations. *Soil Mechanics and Foundation Engineering*, 30(4), 128–135.
- [12] Griffiths, D. V., Fenton, G. A., & Manoharan, N. (2006). Undrained bearing capacity of rough strip footings on spatially random soil using the finite element method. *International Journal of Geomechanics*, 6(6), 421–427. doi: 10.1061/(ASCE)1532-3641(2006)6:6(421).
- [13] Vanmarcke, E. H. (1984). *Random fields, analysis and synthesis*. MIT Press.
- [14] Cafaro, F. & Cherubini, C. (2002). Large sample spacing in evaluation of vertical strength variability of clayey soil. *Journal of Geotechnical and Geoenvironmental Engineering*, 128, 558–568. doi: 10.1061/(ASCE)1090-0241(2002)128:7(558).
- [15] Jha, S. K. (2016). Reliability-based analysis of bearing capacity of strip footings considering anisotropic correlation of spatially varying undrained shear strength. *International Journal of Geomechanics*, 16(5), 06016003. doi: 10.1061/(ASCE)GM.1943-5622.0000638.
- [16] Puła, W., & Chwała, M. (2018). Random bearing capacity evaluation of shallow foundations for asymmetrical failure mechanisms with spatial averaging and inclusion of soil self-weight. *Computers and Geotechnics*, 101, 176–195.
- [17] Kawa, M., & Puła, W. (2020). 3D bearing capacity probabilistic analyses of footings on spatially variable  $c$ - $\phi$  soil. *Acta Geotechnica*, 15(6), 1453–1466. doi: 10.1007/s11440-019-00853-3.
- [18] Wu, Y., Zhou, X., Gao, Y., Zhang, L., & Yang, J. (2019). Effect of soil variability on bearing capacity accounting for non-stationary characteristics of undrained shear strength. *Computers and Geotechnics*, 110(6), 199–210. doi: 10.1016/j.compgeo.2019.02.003.
- [19] Shu, S., Gao, Y., Wu, Y., & Ye, Z. (2021). Undrained bearing capacity of two strip footings on a spatially variable soil with linearly increasing mean strength. *International Journal of Geomechanics*, 21(2), 06020037. doi: 10.1061/(ASCE)GM.1943-5622.0001904.
- [20] Choudhuri, K., & Chakraborty, D. (2025). Stochastic undrained stability analysis of a strip footing over a tunnel on spatially variable clay with rotated soil anisotropy. *Georisk: Assessment and Management of Risk for Engineered Systems and Geohazards*, 20(7), 1–24. doi: 10.1080/17499518.2025.2491098.
- [21] Kawa, M., Puła, W., & Suska, M. (2016). Random analysis of bearing capacity of square footing using the LAS procedure. *Studia Geotechnica et Mechanica*, 38(3), 3–13. doi: 10.1515/sgem-2016-0021.
- [22] Alwalan, M. (2018). Interaction of closely spaced shallow foundations on sands and clays: A review. *International Journal of Advanced Engineering Research and Science*, 5(9), 264269. doi: 10.22161/ijaers.5.9.11.
- [23] Ghazavi, M., & Dehkordi, P. F. (2021). Interference influence on behavior of shallow footings constructed on soils, past studies to future forecast: A state-of-the-art review. *Transportation Geotechnics*, 27, 100502. doi: 10.1016/j.trgeo.2020.100502.
- [24] Ghazavi, M., Foghani, P., & Moghaddam, P. T. (2024). Stochastic analysis for bearing capacity computation of twin strip footings on geogrid-reinforced sands. *Georisk: Assessment and Management of Risk for Engineered Systems and Geohazards*, 18(4), 806–824. doi: 10.1080/17499518.2024.2316263.
- [25] Pieczyńska-Kozłowska, J. M., Chwała, M., & Puła, W. (2023). Worst-case effect in bearing capacity of spread foundations considering safety factors and

- anisotropy in soil spatial variability. *Georisk: Assessment and Management of Risk for Engineered Systems and Geohazards*, 17(2), 330–345. doi: 10.1080/17499518.2022.2046786.
- [26] Boru, Y., Pieczyńska-Kozłowska, J. M., & Puła, W. (2025). Effects of random field heterogeneity of spatial soil properties on the bearing capacity of neighbouring footing *International Journal for Numerical and Analytical Methods in Geomechanics*, 49, 1409–1419. doi: 10.1002/nag.3932.
- [27] Moghaddam, P. T., Dehkordi, P. F., & Ghazavi, M. (2023). Reliability analysis-based safety factor for stability of footings on frictional soils. *Geomechanics and Engineering*, 33(6), 543–552. doi: 10.1680/jgeen.18.00094.
- [28] Khajehzadeh, M. & Keawsawasvong, S. (2024). Artificial intelligence for bearing capacity evaluation of shallow foundation: An overview. *Geotechnical Geological Engineering*, 42, 5401–5424. doi: 10.1007/s10706-024-02863-9.
- [29] Gan, Y., Li, Y., Zhu, H., & Zhang, B. (2025). Resistance factors for design of square foundations on 3D cohesive soils against bearing capacity failure. *Soils and Foundations*, 65(2), 101579.
- [30] Phoon, K. K., Retief, J. V., Ching, J., Dithinde, M., Schweckendiek, T., Wang, Y., & Zhang, L. M. (2016). Some observations on ISO2394:2015 Annex D (Reliability of Geotechnical Structures). *Structural Safety*, 62, 24–33. 10.1016/j.strusafe.2016.05.003.
- [31] Chwała, M., & Kawa, M. (2021). Random failure mechanism method for assessment of working platform bearing capacity with a linear trend in undrained shear strength. *Journal of Rock Mechanics and Geotechnical Engineering*, 13(6), 1513–1530.
- [32] CEN (European Committee for Standardization) (2004) EN 1997-1:2004 Eurocode 7: geotechnical design– part 1: general rules. CEN, Brussels, Belgium.
- [33] Fenton, G. A., & Griffiths, D. V. (2008). *Risk assessment in geotechnical engineering*. John Wiley & Sons. doi: 10.1002/9780470284704.
- [34] Fenton, G. A., & Vanmarcke, E. H. (1990). Simulation of random fields via local average subdivision. *Journal of Engineering Mechanics*, 116(8), 1733–1749. doi: 10.1061/(ASCE)0733-9399(1990)116:8(1733).
- [35] Pieczyńska-Kozłowska, J. M., Puła, W., & Griffiths, D. V. (2015). Influence of embedment, self-weight and anisotropy on bearing capacity reliability using the random finite element method. *Computers and Geotechnics*, 66, 146–156. doi: 10.1016/j.compgeo.2015.02.013.
- [36] Cami, B., Javankhoshdel, S., Phoon, K. K., & Ching, J. (2020). Scale of fluctuation for spatially varying soils: Estimation methods and values. *ASCE-ASME Journal of Risk and Uncertainty in Engineering Systems, Part A: Civil Engineering*, 6(4), 03120002.